1-1-2009

A variable stiffness MR damper for vibration suppression

Xianzhou Zhang
University of Wollongong, xianzhou@uow.edu.au

Weihua Li
University of Wollongong, weihuali@uow.edu.au

Yang Zhou
University of Wollongong, yz248@uow.edu.au

2009 IEEE/ASME International Conference on Advanced Intelligent Mechatronics
Suntec Convention and Exhibition Center
Singapore, July 14-17, 2009

A Variable Stiffness MR Damper for Vibration Suppression

Xianzhou Zhang, Weihua Li, and Yang Zhou

Abstract— **This paper presents the development of a magnetorheological (MR) fluid-based variable stiffness damper and analysis its applications in vibration suppression. The MR fluid isolator used a MR valve control unit and bladders to achieve the variable stiffness and damping in stepless and relative large scope. A mathematical model of the isolator was derived, a prototype of the MR fluid isolator was fabricated and its dynamic behavior was measured in vibration under various applied magnetic fields. The effective stiffness and damping coefficients of the isolator under various magnetic fields were identified and the dynamic performances of isolator were evaluated with simulation. The results demonstrated that the developed MR bladder system can efficiently suppress the structural vibrations.**

I. Introduction

Most of mechanical, civil and construction systems are subjected to excitations that induce vibrations within these systems. These vibrations are usually undesirable, which may damage the systems or even make the systems fail. It is, therefore, of great importance to develop vibration isolation systems to reduce or suppress system vibrations. Vibration isolation systems are generally categorized as passive, active and semi-active modes [1]. The passive mode isolator consists of springs and dampers, which have obtained wide applications because of its simplicity and easy operation. However, such system exhibits an intrinsic limitation that it is effective only in a certain frequency range, off-tuning of which will result in a failure. Many efforts have been conducted to improve the isolation performance over a wide range of frequency by active vibration control. However, active vibration isolation systems are less commonly used than passive systems due to their associated cost, power requirements, complexity and fail-safe problems [1]. Semi-active suspensions can be nearly as effective as fully active suspensions in vibration suppression. They do not require either higher-power actuators or a large power supply. When the control system fails, the semi-active suspension can still work in a passive condition. In early semi-active suspension systems, the adjustable damping force was achieved by using hydraulic semi-active dampers with electromagnetically controlled valves or Friction damper, of which the damping force is controlled by varying the force normal to a friction interface. More recently, the use of smart or intelligent materials, such as PZTs, Shape memory alloys, optical fibres, and ER/MR materials, for development of semi-active isolation systems shows an increasing trend [2]. In particular, the efforts to improve the performance of the isolation systems by using a variable damping damper based on MR fluid has obtained intensive investigations, this is mainly because MR fluid exhibit unique characteristics that their mechanical and rheological properties can be controlled by an external magnetic field [3,4]. Choi et al. proposed a MR fluid-based semi-active isolator using to protect the avionics and sensitive instruments in aircraft and helicopters and studied the performance of the isolator under the control by a skyhook controller [5]. Hiemenz et al. [6] developed dampers in a semi-active seat suspension system for helicopter crew seats to enhance occupant comfort. Spencer et al. [7] and Yoshioka et al. [8] used the MR damper to study seismic response reduction by carrying out a series of earthquake tests. Wang paid attention to enhancing the protection of infrastructure's elements by studying vibration control of a two-span scaled MR damper bridge model [9]. Choi et al. developed a MR mount to reduce the vibration transmitting between engine and vehicle [10]. Yao et al. used a MR damper to develop a semi-active control of vehicle suspension system using skyhook control strategy [11]. Liao and Wang studied the feasibility for improving the ride quality of railway vehicles with semiactive secondary suspension systems using MR dampers [12]. The effectiveness of the proposed concept was evaluated via simulation. Duan et al. implemented a total of 312 MR dampers (Lord Corporation) in a bridge for control of rain-wind-induced cable vibrations [13]. Recently, a few groups made use of MR dampers [14,15] to develop variable damping and stiffness systems, as such systems showed significant improvements in vibration reduction application. Hong et al. [14] did a nice job on the development of a liquid spring shock absorber with controllable MR damping through a bypass comprising tubing and an MR valve. The spring force is developed by compressing the MR fluid hydrostatically due to varying shaft volume. Liu et al. proposed a variable damping and stiffness system using two MR dampers and two springs [15]. By controlling the damping of the MR damper, the total stiffness of this system can be varied in stepless. Meanwhile, due to the fast response characteristic of MR fluid, this system provides the

All authors are with the School of Mechanical, Materials and Mechatronic Engineering, University of Wollongong, Wollongong, NSW 2522, Australia. Contact details of the corresponding author, Dr. Weihua Li, are: phone: 61 2 4221 3490; fax: 61 2 4221 3101; E-mail: weihuali@uow.edu.au.

possibility to apply real time control on it. However, two MR controllable dampers increase the complexity of the system and the fallibility.

In this work, we also make use of the MR valve as a control unit to develop a vibration isolator. As this system includes an MR valve, the damping can be controlled by a magnetic field. Different from the reported techniques in Ref. 14 and 15, the variable stiffness of the system is developed by combining the MR valve control unit with two elastomic bladders.

II. System Design

A. Conceptual Design

The schematic of the proposed MR isolator is shown in Figure 1. The MR isolator consists of an air spring, two connectors, a MR valve and an accumulator. Two connectors link air spring, accumulator and MR valve together with plastic pipes. In each connector, there is a loose non-elastic separate film, which divides the connector into two chambers. The chambers close to the MR valve are filled with MR fluid. The air spring supports the isolated object. Due to the effect of vibration excitation on the isolated object, the air spring is compressed or extended by the isolated object in order to generate the deformation of the air spring, which is the cause of the pressure variation in the air spring. Since the change of the pressure in the air spring, the MR fluid is forced to flow from connector 1 to connector 2 through MR valve. The magnetic field applied to the MR fluid is generated by an electromagnetic coil. The resistance force of the MR fluid is varied by controlling the magnetic field, which thereby varies the characteristics of the isolator, including stiffness and damping.

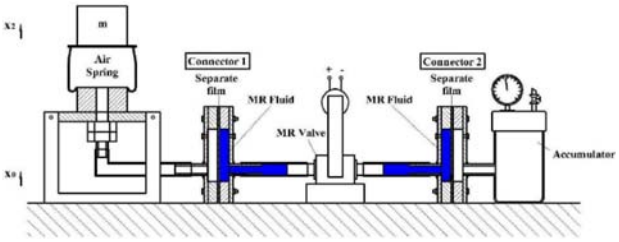

Fig. 1. Schematic of the MRF bladder isolator.

B. Mathematical Model

The lumped model of the developed MR isolator is modeled as a two mass-spring-damper system, as shown in Figure 2a. In this model, k_1 and k_2 are the stiffness of the air spring and the accumulator, respectively, c_0 is the structure damping factor, c_1 is the magnetic field induced damping factor. m_2 is the sprung mass and m_1 is the mass of moving MR fluid. The motion of system is presented by

$$\begin{aligned} m_2\ddot{x}_2 + k_2(x_2 - x_1) + c_0(\dot{x}_2 - \dot{x}_0) = 0 \\ m_1\ddot{x}_1 + k_1(x_1 - x_0) + c_1(\dot{x}_1 - \dot{x}_0) + k_2(x_1 - x_2) = 0 \end{aligned} \quad (1)$$

where x_0 is the input, x_1, and x_2 are displacements of m_1 and m_2. In this design, m_1 is much less than m_2, which is neglected. So equation (1) can be simplified as

$$\begin{aligned} m_2\ddot{x}_2 + k_2(x_2 - x_1) + c_0(\dot{x}_2 - \dot{x}_0) = 0 \\ k_1(x_1 - x_0) + c_1(\dot{x}_1 - \dot{x}_0) + k_2(x_1 - x_2) = 0 \end{aligned} \quad (2)$$

Figure 2b shows the simplified physical model of MR Fluid isolator. In this model, the MR Fluid isolator was simplified into a system which consists of two springs, a controllable MR Fluid damper and structure damping of the isolator. If the damping of the damper is very little when input current applied on the MR valve is zero, two springs k_1 and k_2 can be considered as being in series. The effective stiffness of the system is $k_{eff} = \frac{k_1 \cdot k_2}{k_1 + k_2}$. When the applied current on MR valve is large enough so that the damping force generated by MR valve stop the relative motion between the first layer of the system and foundation, namely x_0=x_1, the mass m_2 is only isolated by k_2. The effective stiffness of the isolation system is k_2. Therefore, when the input current on the MR valve is adjusted in the range between zero and a maximum value, the stiffness can vary from the minimum value to the maximum one, i.e., $\frac{k_1 k_2}{k_1 + k_2} \le k_{eff} \le k_2$.

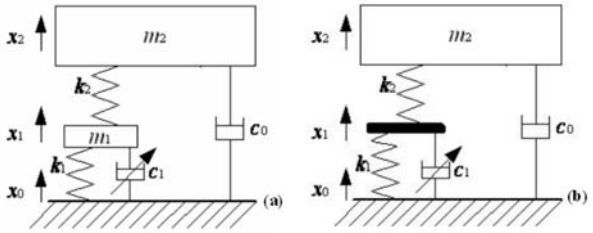

Fig. 2. (a) Schematic model; and (b) simplified model.

C. MR Vavle

As shown in Figure 1 and discussed above, the MR valve is a key element to control the MR fluid flowing status, which consequently vary the system stiffness. As a conventional MR device, this device can basically works as a damping element whose damping capabilities are controlled by an external magnetic field.

The schematic diagram of the MR valve used in this study is shown in Figure 3. The MR valve consists of a C-shaped electromagnet and a fluid gap. The main dimensions of the valve are of L, b and h, where L = 10 mm, active length of fluid gap; b = 10 mm, active width of fluid gap; and h = 4 mm, thickness of fluid gap. The magnetic field produced by a controllable DC power, the inner coil and magnetic pole.

In the absence of magnetic fields, the valve produces the damping force only by the fluid-flowing resistance. When a magnetic field is supplied to the valve, additional damping force due to the yield stress of the MR fluid would be produced.

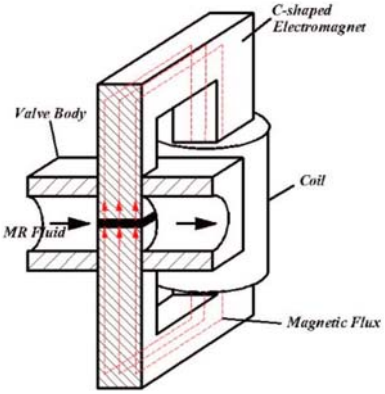

Figu. 3. Schematic of the MR valve.

For the developed MR valve, the damping force, F, is represented as

$$F = c_{eff}\dot{x}_p \tag{3}$$

where $\dot{x}_p$ is the piston velocity and c_{eff} is the equivalent damping coefficient, which is given by

$$c_{eff} = 54599\,I^2 + 13567\,I + 4.13 \tag{4}$$

III. EXPERIMENTAL

A. Experimental Setup

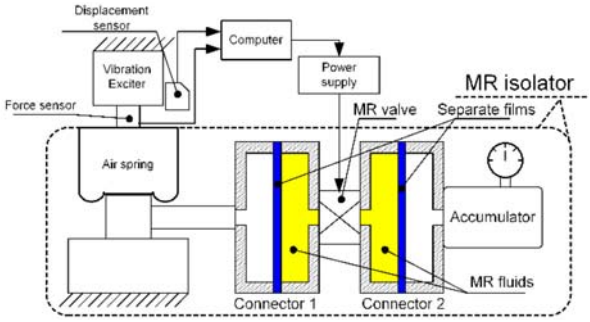

Fig. 4. Experimental setup.

The schematic of the experimental setup is shown in figure 4. The isolator is connected with a vibration exciter (Type: JZK-5, SINOCERA PIEZOTRONICS, INC. China) which generates the vibration for experiments. The vibration signal is generated by the LabVIEW software through a PC and is transmitted to a power amplifier (YE5871-100W) to amplify through the Data Acquisition (DAQ) board (Type: LabVIEW PCI-6221, National Instruments Corporation. U.S.A). After amplifying, the vibration signal is transmitted to vibration exciter. A force sensor (Type: CL-YD-302, SINOCERA PIEZOTRONICS, INC. China) monitors the force F generated by the exciter. The displacement sensor (ILD1700-10) measures the displacement x_2 of the compressed surface of the air spring. The signals from the force sensor and the displacement sensor are amplified by Charge amplifiers (YE5851) and sent to PC via the DAQ board for analysis. A GW laboratory DC power supply (Type: GPR-3030D, TECPEL CO., LTD. Taiwan) is used to provide current to the MR valve for controlling the magnetic field intensity of the isolator and consequently change its dynamic performance.

B. Testing

The maximum force generated by the vibration exciter is 50 N. The initial stiffness of system in absence of any current on the MR valve is 5500N/m, when the air spring is in an open status. Due to the high initial stiffness of the system, it is difficult to carry out the test with large displacement. The maximum displacement in our tests is set as 1 mm. For each test, the vibration exciter is programmed to move forward and backward in a sinusoidal wave at certain displacement amplitudes and frequencies. The resulting forces were measured with the force sensor.

The MR isolator was initially tested without any applied current. Current was then applied to the coils and the MR valve was tested again. The currents varied from 0 to 0.5A, and the experimental data including time, displacement, force, were recorded. All the experiments were carried out at the room temperature of 23℃.

IV. RESULTS AND DISCUSSION

A. Steady State Response

A typical relationship of response force against displacement at the coil current of I = 0.1 A for the first 5 cycles is shown in figure 5. It is found that the displacement cannot reach the amplitude until the second cycle. Therefore, the isolator response could be stable after several cycles. The higher the frequency, the more cycles are needed for the damper response to a stable case. This phenomenon may result from the static friction between different parts of the system.

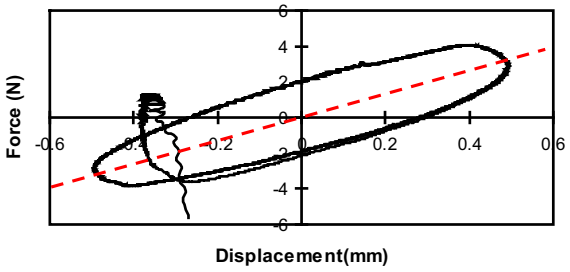

Fig. 5. A typical force-displacement relationship under a magnetic field of 0.1 A

This figure also indicates that the force and displacement form into an elliptical loop. The loop area corresponds to damping energy, thus, the developed system can work as a damper. Also, the damping capability depends on the applied magnetic field, which is similar to conventional MR dampers. However, compared with conventional MR dampers performances under steady state conditions [16-18], this system shows an extinct difference that the long axis of the ellipse (the dashed line) is not horizontal. This means that the system has a stiffness, which equals to the slope the dashed line.

The further study the field induced stiffness and damping capabilities of the developed system, a variety of experiments were conducted. Figure shows the steady state responses of the MR isolator responses at various magnetic fields. All the data are collected from the stable cycle.

It can also be seen from figure 6 that the response force of isolator increases with the increasing magnetic field. The maximum force increases from 2.82 N (input current 0A) to 12.37 N (input current 0.4A). The increase on the response force is more than 4 times. This demonstrates that the system peak damping force shows an increasing trend with the field. Furthermore, the stiffness increment of the system can also be seen from this figure. When the magnetic field increases, the main axis slope increases steadily. Thus, the experimental results demonstrate that the system exhibits variable stiffness and damping capabilities. In addition, the response force varies very little when the input current is greater than 0.4A, which could be due to the saturating magnetization of MR fluid or the valve could be totally blocked when the field is above 0.4A.

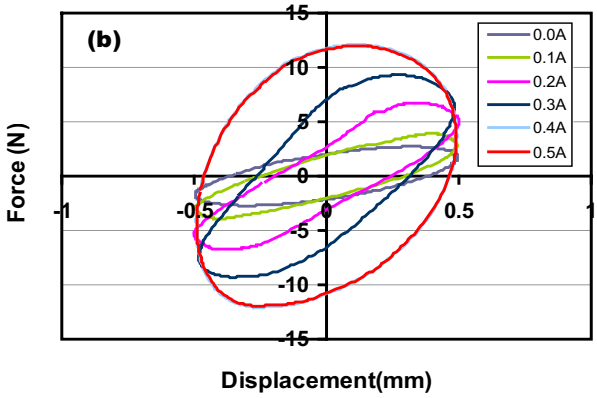

Fig. 6. Steady state responses of force vs. displacement of the MR bladder system under various magnetic fields I=0.0, 0.1, 0.2, 0.3, 0.4, and 0.5A, and X2 = 0.5 mm, f = 0.5 Hz

B. *Effective Stiffness and Damping*

Based on the experimental results, the effective stiffnesses of the system under various magnetic fields were identified by using the same method as in ref. [16-19]. The identified stiffness parameters were shown in figure 7, which demonstrated again the stiffness of the system has more than 4 times increment when the magnetic field increases from 0A to 0.4A.

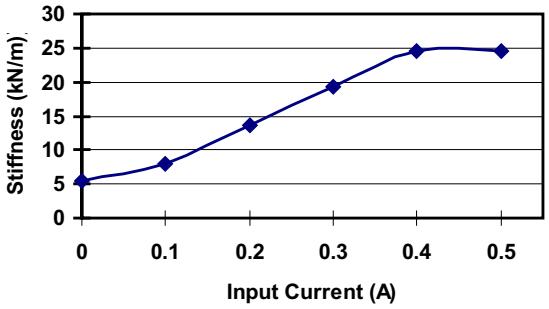

Fig. 7. Effective stiffness versus current.

C. *Simulation*

A simulation was conducted to evaluate the developed MR bladder isolator. In this study, a five-storey fixed-base building was considered and simulated in this study to verify the MRE isolator presented. The model structure has the same structure as considered in ref. [20]. All the parameters of the system have been given in Table 1.

Table 1. Structural model parameters [20, 21]

Level	Floor mass (kg)	Stiffness coefficient (kN/m)	Damping coefficient (kNs/m)
Isolator	m_0=6800	k_0=231.5	c_0=7.45
1st	m_1=5897	k_1=33732	c_1=67
2nd	m_2=5897	k_2=29093	c_2=58
3rd	m_3=5897	k_3=28621	c_3=57
4th	m_4=5897	k_4=24954	C_4=50
5th	m_5=5897	k_5=19059	C_5=38

The rubber bearing isolation system model is a six-degree-of-freedom (6DOF) system. The deformation-force behavior of the MR bladder can be modeled according to the experimental results. Assuming that a large MR bladder has the similar field-dependent behavior to the scaled prototype, but the stiffness of the large bladder is high enough for real applications. The original stiffness of MR bladder was chose as 100kN/m and its stiffness range was fit for the rubber isolator illustrated in reference [20] and [21]. The damping coefficient can be changed from 0.7 to 1.2 according to the experimental results of prototype. The model was established by using a Matlab-simulink program.

To further study the effective of the MR bladder system, similar simulations were also conducted to other two systems, fixed based and the bearing system, as shown in figure 8.

The governing equations of motion are obtained by considering the equilibrium of forces at the location of each degrees of freedom. It is assumed that the relative displacements (x_i), velocities ($\dot{x}_i$) and the ground

accelerations $\ddot{x}_g(t)$ can be measured in real time by the sensors installed in every storey unit. The governing equations of motion are derived as follows

$$m_b\ddot{x}_b + (c_b + c_1)\dot{x}_b - c_1\dot{x}_1 + (k_b + k_1)x_b - k_1x_1 + F_{MR} = -m_b\ddot{x}_g(t),$$
$$m_1\ddot{x}_1 - c_1\dot{x}_b + (c_1 + c_2)\dot{x}_1 - c_2\dot{x}_2 - k_2x_b + (k_1 + k_2)x_1 - k_2x_2 = -m_1$$
$$\cdots\cdots$$
$$m_n\ddot{x}_n - c_n\dot{x}_{n-1} + c_n\dot{x}_n - k_nx_{n-1} + k_nx_n = -m_n\ddot{x}_g(t) \quad (5)$$

where m_n, x_n are the mass, relative displacement with respect to the ground. k_n, c_n are the elastic stiffness coefficient, viscous damping coefficient for the nth storey. k_b, c_b are the original stiffness and damping coefficient of MR bladder without control current. F_{MR} is the control force developed in the MR bladder system, which can be predicted by its mathematical model.

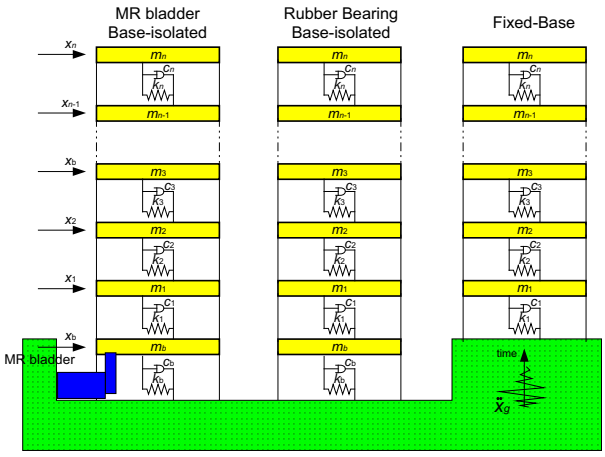

Fig. 8. Idealized structural model [20].

The control strategy based on non-resonance theory was used to control the isolator [22]. The main idea of the algorithm was that the stiffness of system should be increased if the product of drift $x(t)$ and velocity $\dot{x}(t)$ is positive, that is, if $x(t)$ and $\dot{x}(t)$ are in the same direction. By contrast, if $x(t)$ and $\dot{x}(t)$ are opposite to each other, then the stiffness should be decreased. For this simple control algorithm, the long time calculation of feed back signals can be avoid and the real time control can be obtained easily. In this study, the control is designed as

$$i(t) = \begin{cases} 1 & x_b(t)\dot{x}_b(t) > 0 \\ 0 & x_b(t)\dot{x}_b(t) \le 0 \end{cases}$$

$$\text{then } k_{MR}(t) = \begin{cases} 1\times10^5 & x_b(t)\dot{x}_b(t) > 0 \\ 5\times10^5 & x_b(t)\dot{x}_b(t) \le 0 \end{cases} \quad (6)$$

$$\text{and } c_{MR}(t) = \begin{cases} 1.2 & x_b(t)\dot{x}_b(t) > 0 \\ 0.7 & x_b(t)\dot{x}_b(t) \le 0 \end{cases}$$

where $i(t)$ is the control signal.

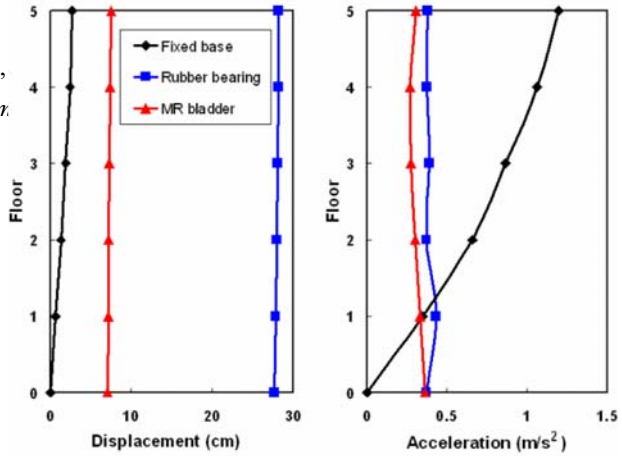

Fig. 9. Peak responses of displacement and accelerations for all levels.

The structure is simulated for the fixed base, the rubber bearing base-isolation, and rubber bearing base-isolation with a semi-active MR bladder. The data of El Centro Earthquake (Time History Data File for North-South Component, time(sec) & Acceleration) has been used to evaluate the control effect of MRE isolator. This record was suggested to explore the effectiveness of the controllers for both actual and amplified intensity to represent moderate and severe vibrations for near and far-fault ground motions. The simulation results are shown in figure 9. It can be seen from this figure, the fixed base structure has large accelerations. However, the rubber bearing isolation system reduced acceleration obviously, but at the expense of increased the displacements. The MR bladder was efficient in reducing the absolute acceleration as well as the displacement responses. It was quite effective in seismic response control as compared to the traditional passive systems.

V. CONCLUSION

In this study, a MR bladder based isolation system, which consists of an air spring, a MR valve and an accumulator, was designed and manufactured. A mathematical model of the MR isolator was developed to show variable stiffness capability. The MR valve performance was experimentally studied. Dynamic performances of the system under various magnetic fields were experimentally studied. Based on experimental results, the effective stiffness and damping coefficients were identified. Both experimental experiments and modeling analysis demonstrated that the system has more than 4 times wide variable stiffness and damping capabilities. The possible application of the device in suppressing building vibrations was simulated. The simulation results indicate that the MR bladder is effective in suppressing the building vibrations.

ACKNOWLEDGMENT

This work was supported by the University of Wollongong through a URC small grant.

REFERENCES

[1] J.Q. Sun, M.R. Jolly, and M.A. Norris, "Passive, adaptive, and active tuned vibration absorbers-a survey," Journal of Mechanical Design, vol. 117B, pp. 234-242, 1995.

[2] G. Song, N. Ma, and H.N. Li, "Applications of shape memory alloys in civil structures," Engineering Structures, vol. 28, pp. 1266-1274, 2006.

[3] X.J. Wang, and F. Gordaninejad, "Flow analysis and Modeling of field-controllable, electro- and magneto-rheological fluid dampers," Journal of Applied Mechanics –Transactions of the ASME, vol. 74, pp. 13-22, 2007.

[4] B. Liu, W.H. Li, P.B. Kosasih, and X.Z. Zhang, "Development of an MR-brake-based haptic device," Smart Materials & Structures, vol. 15, pp. 1960-1966, 2006.

[5] Y.T. Choi, N.M. Wereley, Y.S. Jeon, "Semi-active vibration isolation using magnetorheological isolators," Journal of Aircraft, vol. 42, pp. 1244-1251, 2005.

[6] G.J. Hiemenz, W. Hu, N.M. Wereley, "Semi-active magnetorheological helicopter crew seat suspension for vibration isolation," Journal of Aircraft, vol. 45, pp. 945-953, 2008.

[7] B.F. Spencer, M.K. Sain, and J.D. Carlson, "An experimental study of MR dampers for seismic protection," Smart Materials & Structures, vol. 7 pp. 693-703, 1998

[8] H. Yoshioka, J.C. Ramallo, and B.F. Spencer, "Smart base isolation strategies employing magnetorheological dampers," Journal of Engineering Mechanics, vol. 128, pp. 540-551, 2002.

[9] X. Wang, "Nonlinear behavior of Magnetorheological (MR) fluids and MR dampers for vibration control of structural systems," PhD thesis University of Nevada, Reno, 2002.

[10] S.B. Choi, H.J. Song, H.H. Lee, S.C. Lim, J.H. Kim, H.J. Choi, "Vibration control of a passenger vehicle featuring magnetorheological engine mounts," International Journal of Vehicle Design, vol. 33, pp. 2-16, 2003.

[11] G.Z. Yao, F.F. Yap, G. Chen, W.H. Li, and S.H. Yeo, "MR damper and its application for semi-active control of vehicle suspension system," Mechatronics, vol. 12, pp. 963-973, 2002.

[12] W.H. Liao, and D.H. Wang, "Semiactive vibration control of train suspension systems via magnetorheological dampers," Journal of intelligent material systems and structures, vol. 14, pp. 161-172, 2003

[13] Y.F. Duan, Y.Q. Ni, J.M. Ko, "Cable vibration control using magnetorheological dampers," Journal of Intelligent Material Systems and Structures, vol. 17, pp. 321-325, 2006.

[14] S.R. Hong, G. Wang, W. Hu, and N.M. Wereley, "Liquid spring shock absorber with controllable magnetorheological damping," Proceedings of the Institution of Mechanical Engineers. Part D, Journal of automobile engineering, vol. 220, pp. 1019-1029, 2006.

[15] Y. Liu, H. Matsuhisa, H. Utsuno, and J.G. Park, "Vibration Control by a Variable Damping and Stiffness System with Magnetorheological Damper," JSME International Journal Series C, vol. 48, pp. 305-310, 2006.

[16] W.H. Li, H. Du, N.Q. Guo, "Dynamic behavior of MR suspensions at moderate flux densities," Materials Science and Engineering A, vol. 371, pp. 9-15, 2004.

[17] P. Li, G.M. Kamath, and N.M. Wereley, "Dynamic characterization and analysis of magnetorheological damper behavior," SPIE Conf. on Passive Damping and Isolation (1–5 March, San Diego CA), Paper No.SPIE-3327-25, 1998.

[18] W.H. Li, G.Z. Yao, G. Chen, S.H. Yeo, F.F. Yap, "Testing and Steady State Modeling of a Linear MR Damper under Sinusoidal Loading," Smart Materials and Structures, vol. 9, pp. 95-102, 2000.

[19] V.A. Matsagar, and R.S. Jangid, "Influence of isolator characteristics on the response of base-isolated structures," Engineering Structures, vol. 26, pp. 1735–1749, 2004

[20] K.A. Bani-Hani, and M.A. Sheban, "Semi-active neuro-control for base-isolation system using magnetorheological (MR) dampers," Earthquake Engineering and Structural Dynamics, vol. 35, pp. 1119–1144, 2006.

[21] H. Li, J.P. Ou, "A design approach for semi-active and smart base-isolated buildings," Structural Control and Health Monitoring, vol. 13, pp. 660–681, 2006.

[22] T. Kobori, M. Takahashi, T. Nasu, and N. Niwa, "Seismic response controlled structure with active variable stiffness system," Earthquake Engineering and Structural, vol. 22, pp. 925-941, 1993.